# Higher order mode conversion via focused ion beam milled Bragg gratings in Silicon-on-Insulator waveguides

**V.G. Ta'eed*, D.J. Moss and B.J. Eggleton**

*CUDOS, School of Physics, The University of Sydney, Sydney, NSW 2006, Australia*
*http://www.physics.usyd.edu.au/cudos/*
*(*) also CSIRO Industrial Physics, PO Box 218, Lindfield, NSW 2070, Australia*
*egg@physics.usyd.edu.au*

**D. Freeman, S. Madden, M. Samoc and B. Luther-Davies**

*CUDOS, Laser Physics Centre, The Australian National University, Canberra, ACT 0200, Australia*

**S. Janz and D.-X. Xu**

*Institute for Microstructural Sciences, National Research Council of Canada, Ottawa, Ontario, Canada*

**Abstract:** We report the first Bragg gratings fabricated by Focused Ion Beam milling in optical waveguides. We observe striking features in the optical transmission spectra of surface relief gratings in silicon-on-insulator waveguides and achieve good agreement with theoretical results obtained using a novel adaptation of the beam propagation method and coupled mode theory. We demonstrate that leaky Higher Order Modes (HOM), often present in large numbers (although normally not observed) even in nominally single mode rib waveguides, can dramatically affect the Bragg grating optical transmission spectra. We investigate the dependence of the grating spectrum on grating dimensions and etch depth, and show that our results have significant implications for designing narrow spectral width gratings in high index waveguides, either for minimizing HOM effects for conventional WDM filters, or potentially for designing devices to capitalize on very efficient HOM conversion.



**OCIS codes:** (050.2770) Gratings; (130.3120) Integrated optics devices

## References and links

1. *Topics in Applied Physics, vol 94: Silicon Photonics*, Lorenzo Pavesi and David J. Lockwood, ed. (Springer-Verlag Heidelberg, 2004).
2. R.A. Soref, J. Schmidtchen, and K. Petermann, "Large Single-Mode Rib Waveguides in GeSi-Si and Si-on-$SiO_2$," IEEE J. of Quant. Elec., **27,** 1971-1974 (1991).
3. M. Lončar, T. Doll, J. Vučković, and A. Scherer, "Design and fabrication of silicon photonic crystal optical waveguides," J. Lightwave Technol. **18,** 1402-1411 (2000).
4. R. Claps, D. Dimitropoulos, V. Raghunathan, Y. Han, and B. Jalali, "Observation of stimulated Raman amplification in silicon waveguides," Opt. Express, **11**, 1731-1739 (2003), http://www.opticsexpress.org/abstract.cfm?URI=OPEX-11-15-1731.
5. R.E.Slusher and B.J.Eggleton, *Nonlinear Photonic Crystals* (Springer, 2003), pg 169.
6. D.Wiesmann, C.Germann, D.Erni, and G.L.Bona, "Apodized surface-corrugated gratings with varying duty cycles," Photon. Technol. Lett., **12,** 639-641 (2000).
7. T.E.Murphy, T.Hastings, and H.I.Smith, "Fabrication and characterization of narrow-band Bragg-reflection filters in silicon-on-insulator ridge waveguides" J. Lightwave Technol., **19,** 1938-1942 (2001).
8. J.Canning, D.J.Moss, M.Faith, P.Leech, P.Kemeny, C.V.Poulsen, and O.Leistiko, "Ultrastrong UV written gratings in PECVD grown germanosilicate rib waveguides," Electron. Lett. **32,** 1479-1480 (1996).
9. C.D. Poole, J.M. Wiesenfeld, D.J. DiGiovanni, A.M. Vengsarkar, "Optical fiber-based dispersion compensation using higher order modes near cutoff," J. Lightwave Technol., **12,** 1746-1758 (1994).
10. T. Erdogan "Fiber Grating Spectra," J. Lightwave Technol., **15**, 1277-1294 (1997)

#5160 - $15.00 US Received 31 August 2004; revised 13 October 2004; accepted 14 October 2004

11. B.J.Eggleton, P. S. Westbrook, C. A. White, C.Kerbage, R.S.Windeler, and G.L.Burdge, "Cladding-mode-resonances in air-silica microstructure optical fibers," J. Lightwave Technol., **18,** 1084-1100 (2000).
12. M.D. Feit and J.A. Fleck, "Computation of mode properties in optical fiber waveguides by a propagating beam method," Appl. Opt., **19,** 1154-1164 (1980).
13. RSoft Design Group Inc., *BeamPROP, 5.1.1* (RSoft Design Group Inc, 2003), pg. 17-19.
14. J.J. Villa, "Additional data on the refractive index of silicon," Appl. Opt. **11,** 2102-2103 (1972).
15. A. Othonos and K Kalli, *Fiber Bragg Gratings* (Artech House, 1999), pg. 95-105
16. Po Shan Chan, H. K. Tsang, and C. Shu, "Mode conversion and birefringence adjustment by focused-ion-beam etching for slanted rib waveguide walls," Opt. Lett., **28,** 2109-2111 (2003).
17. D.B. Stegall and T. Erdogan, "Leaky Cladding Mode Propagation in Long-Period Fiber Grating Devices," Photon. Technol. Lett., **11,** 343-345 (1999).

## 1. Introduction

In the last decade, silicon photonics has become an attractive platform for creating integrated optical devices [1] due to its high refractive index (3.5 compared to 1.5 in silica), its transparency in the 1500-1600 nm telecommunications window, and mature fabrication processes. More recently, the availability of high quality Silicon-on-Insulator (SOI) substrates for the microelectronics industry has provided a convenient and inexpensive medium for photonics for not only waveguides [2] but also photonic crystal structures [3]. This in turn has provided further impetus to investigate nonlinear processes, such as Raman nonlinearities [4], with the potential for more complex active devices.

However, whilst the large refractive index of silicon offers many advantages it poses significant challenges for fabricating narrow spectral width Bragg gratings, of interest not just for WDM filters but for many nonlinear optical processes [5]. The reason for this is that the lack of photosensitivity in silicon means that grating structures must be realized through a periodic modulation in waveguide core dimensions [6]. Because of the very large core/cladding refractive index difference in silicon waveguides this tends to create a very strong grating index modulation and hence broad spectral widths. Consequently, despite the plethora of recent work in 2D photonic crystals in SOI, narrow spectral width gratings in SOI waveguides have only recently been reported [7].

In this paper we report the first use of focused ion beam (FIB) milling to fabricate gratings in an optical waveguide and demonstrate narrow spectral width gratings in SOI waveguides. We use FIB milling, a powerful technique allowing flexible, direct writing of nanometer resolution features without the need for etching, to fabricate shallow, weak index modulation surface relief gratings in rib waveguides. These grating properties allow us to demonstrate a number of unique features. First, we achieve narrow spectral width gratings because of the relatively weak index modulation of the shallow surface grating profile created by the FIB. Secondly, we demonstrate very efficient coupling to very high order modes (HOM) because of the very strong overlap of these modes with the shallow surface gratings. Third, by detailed comparison with theory we show that these gratings can be a powerful diagnostic of waveguide modes, and particularly of leaky HOM that are typically hard to observe.

Although it has been known for some time [2] that high index waveguides can be single moded even for large waveguide dimensions (where the corresponding 2D slab waveguide would be highly multimoded), the fact that HOM are still present in these waveguides in the form of leaky modes is less well understood. These leaky HOM are typically hard to observe because of the difficulty in coupling to them as well as their lossy nature, and we show that gratings can be a very powerful diagnostic of them. Our results are also remarkable in that we achieve almost complete suppression of the fundamental Bragg transmission dip. This occurs because of the much larger overlap of the shallow surface grating with the HOM than the fundamental mode. This is in contrast with bulk photosensitive gratings[8], where the effect of HOM, or cladding modes, is comparatively weaker because of the large overlap between the grating and the fundamental guiding mode.

#5160 - $15.00 US Received 31 August 2004; revised 13 October 2004; accepted 14 October 2004

We employ a novel application of beam propagation method (BPM) and coupled mode theory (CMT) to calculate the grating transmission spectrum and achieve good agreement with experiment for the grating resonance wavelengths and overall trend in grating strengths. We then show that the dependence of grating spectra on waveguide and grating parameters have significant implications for grating designs based on modulation of physical waveguide dimensions, both in challenges to reduce the effects of leaky HOM for WDM filters, and in opportunities for devices based on higher order mode conversion – potentially much higher order than what is typical in fiber [9].

The rest of this paper is structured as follows. Section 2 covers device fabrication, Section 3 presents the experimental optical characterization results, Section 4 outlines the theory of the grating spectral profiles using BPM and coupled mode theory and Section 5 compares the theoretical and experimental results and further investigates the dependence of grating spectral profile on waveguide and grating parameters.

## 2. Device fabrication

The rib waveguides were fabricated from 5 μm thick SOI substrates, over a 0.5 μm thick silica buffer layer by standard photolithography and reactive-ion etching. Our substrates were then cut and polished, yielding 2 cm long waveguides with propagation losses of 0.5dB/cm and a fiber coupling loss of 2.5 dB/facet. Figure 1 shows the rib waveguide dimensions along with a scanning electron microscope (SEM) cross-section of the waveguide. Soref *et al*. [2] have shown that rib waveguides in high index materials such as silicon can be single moded even for waveguide dimensions much larger than the propagating wavelength, where the corresponding two dimensional slab waveguide would be highly multi-moded. The single mode conditions are [2],

$$\frac{W}{H} \le \alpha + \frac{h/H}{\sqrt{1-(h/H)^2}}, \tag{1}$$

$$\frac{h}{H} \ge \frac{1}{2}, \tag{2}$$

where, W, H and h define the respective width, total rib height and slab height of the rib waveguide and α is a fitting constant, determined to be approximately 0.3. Single mode operation can be achieved, even for large rib waveguides, because of the comparatively weak lateral effective index guidance of higher order modes in the lateral direction. Modes with more than one lobe in the vertical direction will strongly couple into guided slab modes and will therefore become leaky. The dimensions of our waveguides fall within the boundary of the requirements for single mode operation.

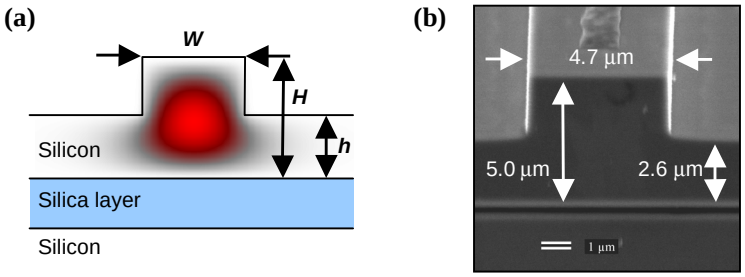


Fig. 1. Cross-sectional profile of a rib waveguide: (a) a schematic, showing simulated mode profile for the fundamental mode and (b) a scanning electron micrograph of the waveguide used in this paper.

#5160 - $15.00 US Received 31 August 2004; revised 13 October 2004; accepted 14 October 2004

In order to fabricate the surface relief gratings, shallow grooves were milled in the waveguide surface (Fig. 2(a)) with a research grade FIB system, combining an Orsay Physics Canion 31M Plus FIB, with a JEOL JSM-6460LV scanning electron microscope (SEM). The FIB is mounted at an angle of 55º to the SEM column, and the sample can be rotated to face either beam. The FIB produces a tightly focused beam of Ga+ ions which can be deflected electronically over a field size of over 0.5 mm, controlled via an external analogue input.

Gratings were milled with a FIB aperture of 20 µm, a beam energy of 30 keV, a beam current of 12 pA and spot size of below 20 nm. Typical exposure time was 20 minutes for a 330 µm long x 6.5 µm wide grating, which was chosen to be shorter than the maximum field size in an attempt to mitigate any distortion near the field boundary. The gratings were positioned 5mm from one of the waveguide facets, and had a pitch of 240 nm (with ~50% duty cycle) to yield a fundamental Bragg wavelength near 1665 nm.

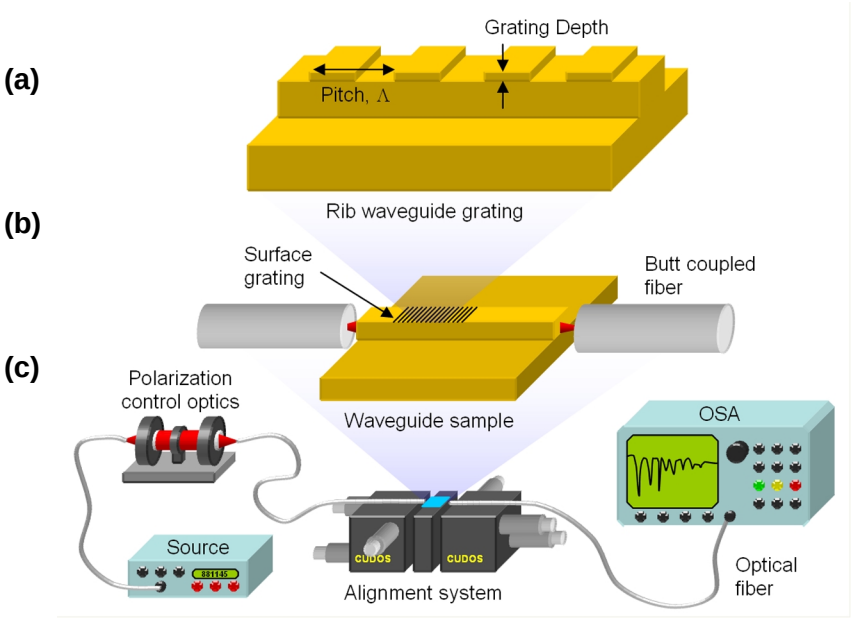


Fig. 2. Experimental setup: (a) the FIB milled rib grating structure, (b) coupling to the grating waveguide, and (c) measuring the optical grating transmission spectrum.

## 3. Experiment

Following fabrication of the gratings the devices were optically characterized (Fig. 2(c)) using a broadband (un-polarized) Light-Emitting-Diode (LED) source and optical spectrum analyzer (OSA) both having a wide spectral range (1300 nm to 1700 nm). The large rib waveguide design allowed simple butt-coupling to standard single mode fiber as shown in Fig. 2(b). An in-fiber polarizer was used to provide polarization control, and for some measurements a narrower spectral width EDFA ASE source was used to provide better signal to noise.

Whilst Bragg gratings operating on resonance with the fundamental mode can easily be observed in either reflection or transmission (as a peak resonance or loss dip, respectively), when coupling to HOM they are more easily characterized in transmission (where the grating results in a loss spectra) because the reflected HOMs do not couple back into fibre and hence are difficult to observe. Therefore in this paper we focus on the transmission loss spectra to characterize our gratings.

#5160 - $15.00 US Received 31 August 2004; revised 13 October 2004; accepted 14 October 2004

Figure 3 shows the resulting experimental transmission loss spectra for unpolarized light from 1300nm to 1700nm of a uniform grating. These results display a number of dramatic and unexpected features, the most remarkable of which is the near absence of any significant grating resonances near the expected Bragg wavelength of 1665nm. Also surprising is the presence of many strong (up to 12 dB) grating resonances right through the 400 nm wavelength range. This is in contrast to UV written Bragg gratings in fiber, where the fundamental Bragg resonance dominates higher order cladding mode resonances [9, 10].

Figure 4 shows a higher resolution (80 pm) spectrum, taken with an EDFA ASE source and an in-fiber polarizer, of the 1532 nm and 1554 nm transmission resonances. The TE / TM spectral shift is less than 0.1 nm, indicating low birefringence. On the other hand, the polarization dependent loss is larger with the TE peak being stronger (12 dB) than the TM (6 dB). From standard coupled mode theory, a 12 dB reflection from a 330 μm long uniform grating corresponds to a coupling coefficient ($\kappa_i$) of 62 $cm^{-1}$ and should have a spectral width of 1.9 nm. The broader FWHM (3dB) widths we observe of 5-6 nm are possibly due to induced chirp created by residual distortion of the FIB pattern across the writing field and is subject to further investigation. In order to understand these experimental results, we developed a hybrid combination of beam propagation method and coupled mode theory to calculate the optical grating spectrum.

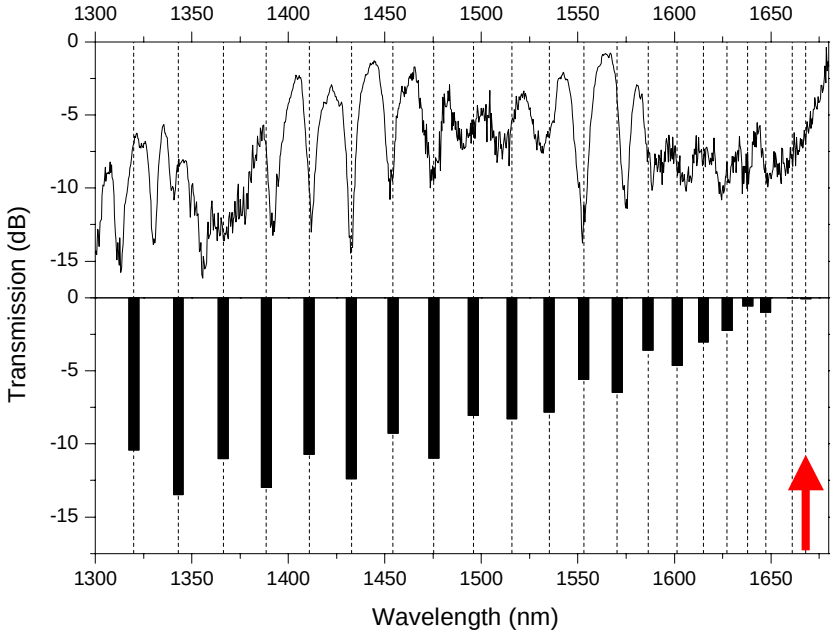


Fig. 3. Experimental (top) and theoretical (bottom) optical transmission spectrum of the surface grating from 1300 nm to 1680 nm using an unpolarized LED and optical spectrum analyzer with 0.4 nm resolution. The dotted lines are an aid to the eye, and the red arrow indicates the position of the fundamental Bragg resonance.

#5160 - $15.00 US Received 31 August 2004; revised 13 October 2004; accepted 14 October 2004

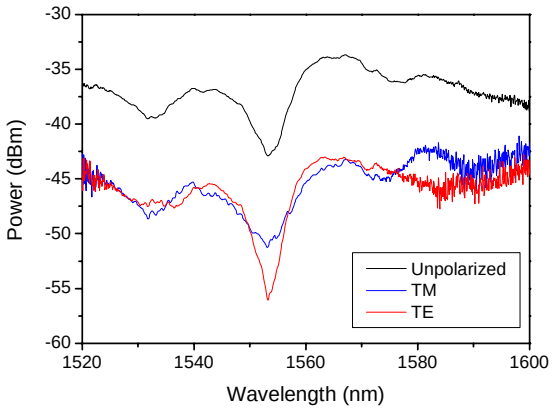


Fig. 4. Grating transmission spectrum for the 1532 nm and 1554 nm resonances measured with a high power ASE-EDFA source for both TE and TM polarizations at a resolution of 80 pm.

## 4. Theory

### *4.1 Bragg-grating coupling to HOM*

In this section, we develop a novel approach based on a BPM algorithm previously used [11] to quantitatively predict the location and relative strength of HOM resonances and modes in lossy waveguides [12]. The phase matching condition for scattering by a Bragg grating of a forward propagating incident mode into a backward propagating mode, given by $\beta_{scat} = \beta_{inc} + K$ (where $\beta_{inc} = 2\pi n_{inc}/\lambda$ and $\beta_{scat} = 2\pi n_{scat}/\lambda$ are the respective incident and scattered wavevectors, K is the grating wavevector ($K = 2\pi/\Lambda$) where $n$ is the effective modal index of the respective mode and $\Lambda$ is the grating pitch) yields the Bragg equation:

$$\lambda = \Lambda\left(n_{inc} + n_{scat}\right), \tag{3}$$

for the wavelengths at which resonances occur in the grating spectrum – either as peaks in reflection or as dips in transmission. For short period gratings, scattering can be either *diagonal*, when the incident and scattered modes only differ in propagation direction, or *off-diagonal*, where the two modes are different (as well as propagating in opposite directions). For the single mode rib waveguides considered here, only the fundamental mode is significantly excited due to the low overlap of the HOM with the fundamental launched fiber mode. Therefore we expect that the grating spectra will contain one diagonal solution (forward to reverse propagating fundamental) and many off-diagonal solutions (forward propagating fundamental mode to the backward propagating HOM) which will manifest as dips in transmission. As mentioned above, in practice it is much more difficult to observe HOM resonances in reflection than transmission since this relies on coupling of the HOM back into fiber, whereas transmission dips only rely on resonantly coupling the light out of the fundamental mode via the Bragg grating.

### *4.2 Coupled mode analysis*

From coupled mode theory [11, 15], the transmission at the resonant wavelength through a uniform (unapodized, unchirped) grating is given by:

$$T_i = 1 - \tanh^2(\kappa_i L), \tag{4}$$

where $L$ is the grating length and $\kappa_i$ is the coupling coefficient linking the fundamental mode ($E_0(x,y)$) and the $i^{th}$ scattered mode ($E_i(x,y)$). The $\kappa_i$ are proportional to the overlap integral

#5160 - $15.00 US Received 31 August 2004; revised 13 October 2004; accepted 14 October 2004

between the incident and scattered mode fields and the transverse spatial distribution of the grating refractive index perturbation ($\Delta n(x,y)$):

$$\kappa_i = \left(\frac{\pi}{\lambda}\right)\iint \Delta n(x,y) E_0(x,y) E_i^*(x,y) dxdy \,. \tag{5}$$

In this paper, we define the grating refractive index perturbation as $\Delta n(x,y) = \Delta n \times G(x,y)$, where $\Delta n$ is the index difference between the waveguide material (silicon) and the cladding (air) shown schematically in Fig. 2(a), while $G(x,y)$ describes the transverse spatial distribution of the grating which we approximate to be a step function.

Whilst in principle the spectra for a surface grating can be calculated from coupled mode equations (given the modes of the system) this is difficult for high index contrast waveguides due to the large number of modes involved. For this reason we use a numerical technique based on BPM.

*4.3 Correlation mode solving approach*

The correlation mode-solving technique is particularly suited to solving for eigenpairs of structures that contain a large number of either guiding and/or leaky cladding modes. We use this technique to obtain the Bragg grating spectrum as follows [11]. First, instead of launching an arbitrary field as is typically done in BPM calculations, we launch a field given by the profile of the grating and the fundamental mode:

$$E(x,y,0) = \Delta n(x,y) E_0(x,y) \,. \tag{6}$$

This is closely related to Eq. (5) and gives rise to a simple intuitive picture. The BPM launch field can be seen to emulate the Bragg grating - effectively launching the incident field into the waveguide - as the grating does in reality from the incident optical field. As in conventional BPM, the correlation function between the input and propagating fields:

$$P(z) = \iint E(x,y,0) E^*(x,y,z) dxdy \,, \tag{7}$$

is computed during propagation. A Fourier transform of this correlation function results in a *mode spectrum* with sharp peaks of amplitude $\alpha_i$, whose positions identify the modal effective indices, $n_i$. By computing the Fourier transform of $E(x,y,z)$ evaluated at $n_i$, the modal fields can be calculated [11-13]. The difference in our case is that the position of the peaks now represent the propagation constants of those modes which are excited by the grating and the strength of those peaks, $\alpha_i$ , are directly proportional to the coupling coefficients:

$$\alpha_i = \left(\frac{\lambda}{\pi}\right)\kappa_i \,. \tag{8}$$

For Bragg gratings written in typical fibers this would normally be enough to determine the Bragg grating strengths and resonance wavelengths since the core/cladding refractive index difference is small enough (at most a couple of percent) to neglect mode dispersion. However, in silicon the large refractive index contrast means the higher order modes extend over hundreds of nanometers in wavelength, requiring that both waveguide and material dispersion be accounted for and this results in Eq. (3) becoming a transcendental equation. To solve Eq. (3) for the diagonal Bragg wavelengths we first solve for the waveguide mode effective indices at selected wavelengths over the spectral range of interest and then interpolate to obtain continuous functions (Fig. 5), accounting for material [14] dispersion. The Bragg wavelengths for diagonal terms are then given by the intersection of the $\lambda/2$ line with the effective mode indices (Fig. 5) and are obtained iteratively. The off diagonal terms, given by the phase matching condition, Eq. (3), are obtained by finding the corresponding intersections of $\lambda/2$ with plots of ($n_{inc}$ + $n_{scat}$ ). Finally, Eq. (8) is used to convert the amplitudes of the peaks in the mode spectrum into coupling strengths at the wavelengths

#5160 - $15.00 US Received 31 August 2004; revised 13 October 2004; accepted 14 October 2004

where the BPM calculations are performed, and a simple interpolation is then used to obtain the strengths at arbitrary wavelengths. For the BPM launch condition given in Eq. (6) we use a uniform rectangular field 5 μm wide and 40 nm deep, chosen to approximate the overlap of the shallow surface grating and planar fundamental mode field.

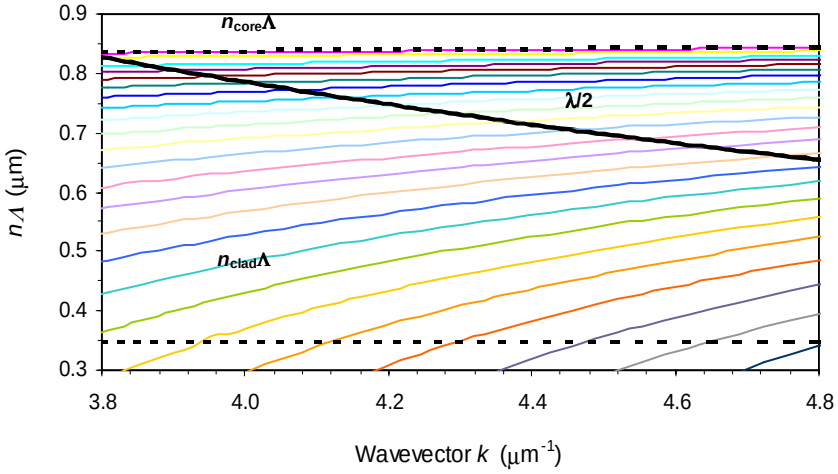


Fig. 5. Effective index versus wavevector of the first 24 TE modes of the rib waveguide are represented by the colored lines. Intersection with the thick black line (λ/2) indicates a diagonal solution of the Bragg equation.

## 5. Results and discussion

Figure 3 compares the theoretical (bottom) and the experimental (top) transmission spectrum of the grating arising from scattering from the fundamental mode to the first 21 HOM. We see that there is good agreement with the grating resonance wavelengths except for a few of the very shortest wavelength peaks. The theory also predicts a number of features observed in the experimental grating strengths, including the near absence of resonances near the fundamental Bragg mode at 1665 nm, and the dominance of dips arising from coupling to very HOM. This is in stark contrast to cladding mode resonances in fiber that are typically much weaker than the fundamental Bragg peak [15]. We characterized the grating surface relief profile by atomic force microscopy (AFM), and found the depth of the surface modulation to be less than 10nm. This is a strong indication that a significant fraction of the index change is in fact due to either doping or implantation damage from the $Ga^+$ ions, and is the subject of further investigation. The residual discrepancy between theory and experiment could be either due to these effects or the fact that the very shallow grating depth of 40 nm is probably near the limit of what the BPM method is capable of, given the paraxial approximation.

Figure 6 shows the theoretical mode profiles of the first 20 HOM of our rib waveguide at 1550nm. The field amplitude of the HOM at the surface where the grating is located is much larger than for the fundamental mode, resulting in higher overlap. For our situation of relatively large, high index waveguides with shallow surface gratings, this results in the extreme situation where the fundamental Bragg resonance (and indeed even the first few HOM resonances) are nearly absent, whereas the cross-coupling resonances from the fundamental to very high order modes is quite large.

#5160 - $15.00 US Received 31 August 2004; revised 13 October 2004; accepted 14 October 2004

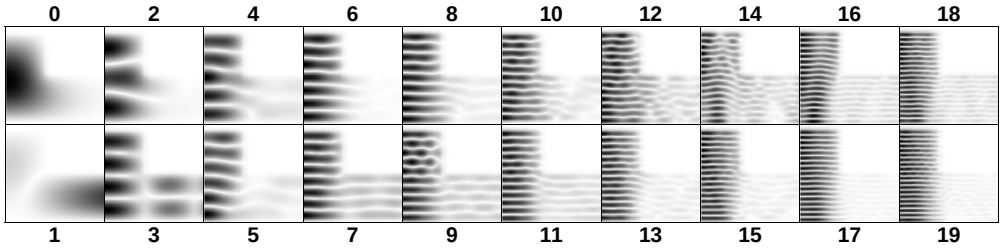


Fig. 6. Mode profiles for the first 21 modes of the rib waveguide. As the mode profiles are horizontally symmetric, only the right half of each profile is displayed

This level of agreement between theory and experiment lends confidence to the correlation mode-solving BPM method, and suggests further analysis of these HOM to understand more subtle features in the spectra, such as the oscillations in grating resonance strengths in Fig. 3. Fig. 7(a) shows the theoretical grating coupling strengths and Fig. 7(b) shows the mode loss for the HOM. Whilst the grating strength is determined primarily by the spatial overlap with the HOM, the oscillations can be seen to correlate with oscillations in mode loss. This is not unexpected since modes with higher loss occupy a larger volume and consequently have a reduced grating interaction. The origin of these oscillations is, however, not immediately obvious. We find it arises from variation in matching between the mode profile in the central rib region and the surrounding slab waveguide. Modes that have vertical profiles in the rib region that closely match the slab region couple more efficiently to radiating 2D modes and hence have higher loss.

If we approximate the width of the mode lobes in the vertical direction ($\eta_i$) in the central rib waveguide region as $\eta^{rib}_i \approx H / (N+1)$, where N is an integer (equal to the mode number), and in the surrounding slab region by $\eta^{slab}_i \approx h / (M+1)$, where M is also an integer (not necessarily equal to the mode number), one might expect modes with comparable (vertical) lobe sizes in both regions ($\eta^{rib}_i \approx \eta^{slab}_i$) to couple more strongly and thus have higher losses. Figure 8 shows a schematic representation of a figure of merit, defined to be "1" for optimal matching, $\eta^{rib}_i \approx \eta^{slab}_i$ ( = h / (M+1)), and "0" for minimum matching ( $\eta^{rib}_i \approx h / (M+½)$ ). Figure 7(c) shows a plot of this figure of merit for each mode. The strong correlation between matching of rib and slab modes and mode loss, and then ultimately Bragg grating strength, implies that grating strengths can be engineered by choosing the appropriate etch depth to yield the desired mode loss.

#5160 - $15.00 US Received 31 August 2004; revised 13 October 2004; accepted 14 October 2004

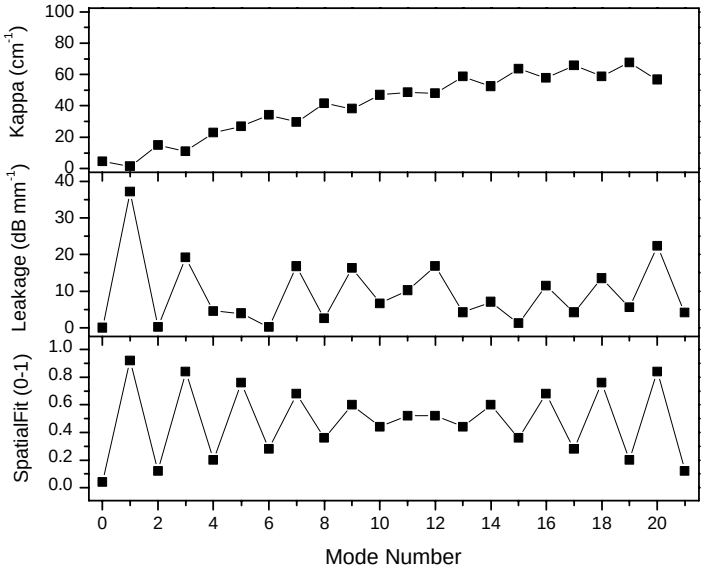


Fig. 7. (a) Top: Bragg grating coupling coefficient of the first 21 modes of the rib waveguide (b) Middle: leakage rates of the HOM as measured from BPM simulations and (c) Bottom: figure of merit representing how well the mode lobes fit in the both rib and slab regions (0.0 = poor, 1.0 = good spatial overlap).

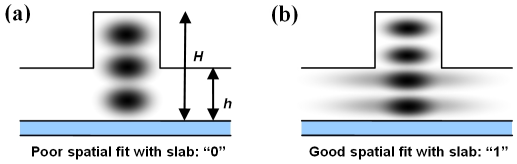


Fig. 8. Schematic representation of the spatial overlap of the mode with the slab region. For modes that do not fit an integer number of lobes (a) in the slab, the figure of merit is defined as "0", while for modes that fit an integer number of lobes in the slab (b) and hence have good overlap with the slab, the figure of merit is defined to be "1".

Grating dimensions also have a significant influence on the grating spectra and Fig. 9 shows theoretical spectra for gratings with depths of 40 nm, 200 nm and 400 nm, respectively. The 400 nm deep grating couples significantly more to lower order modes and these modes dominate the spectrum. For WDM filters one would need to minimize the effects of HOM by designing gratings with larger overlap to the fundamental mode either by having deeper gratings or using novel geometries such as holes milled from the side near the base of the rib, for example. This would be readily achievable with FIB milling.

Finally, the presence of HOM in rib waveguides also raises the interesting possibility for novel HOM devices [16] similar to what has been reported in fiber [9], with the potential to couple to much higher order (albeit lossy) modes. These devices could be used either in linear applications exploiting the higher dispersion of the HOMs, or in a nonlinear fashion by coupling the fundamental mode into a HOM where the field spreads further into cladding regions that may contain complex nonlinear structures [17].

#5160 - $15.00 US Received 31 August 2004; revised 13 October 2004; accepted 14 October 2004

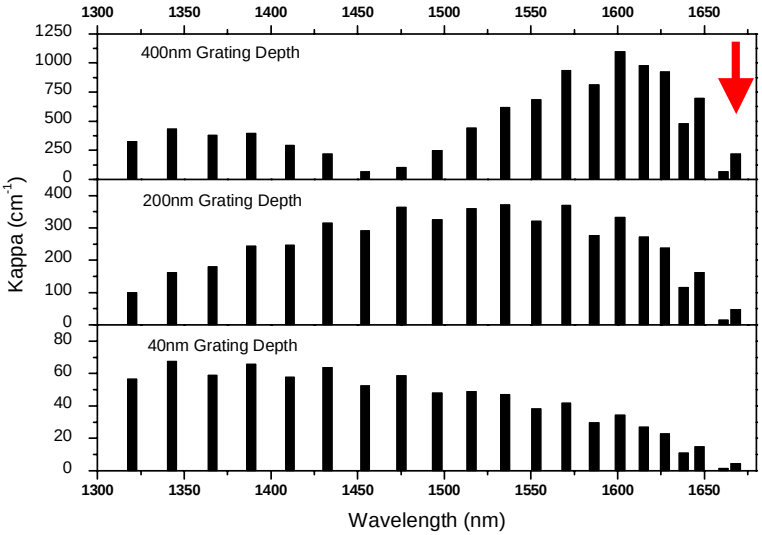


Fig. 9. Theoretical coupling coefficients (κ) for grating depths of 40nm, 200nm and 400 nm. The overall envelop increases in strength and shifts to longer wavelength (and lower order modes) as the grating probes more of the fundamental mode. The arrow at the top right indicates the position of the fundamental grating resonance.

## 6. Conclusions

We report the first Bragg gratings fabricated by FIB milling in SOI optical waveguides. We demonstrate surface relief gratings in rib waveguides and observe dramatic spectral features that include a near absence of the fundamental Bragg peak and a complete domination of the grating spectra by peaks arising from resonant coupling to very high order modes. These HOM are normally not observed in single mode rib waveguides but can in fact dominate the grating spectra when their overlap with the shallow surface relief grating is much larger than the fundamental mode. We achieve good agreement with theory, and find that the Bragg wavelengths and strengths depend not only on overall waveguide and grating dimensions but the waveguide etch depth relative to rib height. Our results have significant implications for grating devices both as WDM filters, and devices based on waveguide converters to very high order modes.

## Acknowledgments

This work was produced with the assistance of the Australian Research Council (ARC) under the ARC Centres of Excellence Program. CUDOS (the Centre for Ultrahigh-bandwidth Devices for Optical Systems) is an ARC Centre of Excellence.

#5160 - $15.00 US Received 31 August 2004; revised 13 October 2004; accepted 14 October 2004